Dynamic exergetic performance assessment of an integrated solar pond

Mehmet Karakilcik*

Department of Physics,
Faculty of Sciences and Letters,
University of Çukurova,
Adana 01330, Turkey
Email: kkilcik@cu.edu.tr
*Corresponding author

Ismail Bozkurt

Department of Mechanical Engineering,
Faculty of Engineering,
University of Adiyaman,
Adiyaman 02040, Turkey
Email: ibozkurt@adiyaman.edu.tr

Ibrahim Dincer

Faculty of Engineering and Applied Science,
University of Ontario Institute of Technology (UOIT),
2000 Simcoe Street North,
Oshawa, Ontario L1H 7K4, Canada
Email: Ibrahim.Dincer@uoit.ca

Abstract: In this paper, we present an experimental investigation of the exergetic performance of a solar pond integrated with solar collectors (with a surface area of 2096 m^2 and a depth of 2 m, and four flat-plate collectors with dimensions of 1.90 m × 0.90 m). A data acquisition device is used to measure and record the temperatures hourly at various locations in the pond. An exergy model is developed to study the dynamic exergetic performance of the solar pond integrated with solar collectors in terms of exergy efficiencies which are then compared with the corresponding energy efficiencies. Thus, the energy efficiencies are found to be 21.33%, 23.59%, 24.28% and 26.52%; the exergy efficiencies are found to be 20.02%, 21.66%, 22.24% and 23.84% for using 1, 2, 3 and 4 collectors, respectively. The energy efficiencies are compared with the corresponding exergy efficiencies.

Keywords: solar energy; thermal energy; ISP; integrated solar pond; energy and exergy efficiency.

Reference to this paper should be made as follows: Karakilcik, M., Bozkurt, I. and Dincer, I. (2013) 'Dynamic exergetic performance assessment of an integrated solar pond', *Int. J. Exergy*, Vol. 12, No. 1, pp.70–86.

Biographical notes: Mehmet Karakilcik works as an Associate Professor in Department of Physics at Cukurova University in Adana, Turkey since 1999. He served as an Assistant Manager of Space Sciences and Solar Energy Research and Application Center at Cukurova University from 2003 to 2011. His research areas are solar pond, solar energy storage and heating systems, mathematical models, energy and exergy analyses of solar ponds and integrated solar pond systems.

Ismail Bozkurt works as a Physics Teacher since 2006. He received his MSc and PhD degrees from Cukurova University in Adana, Turkey. His areas of research are thermal energy storage systems and exergy analyses of integrated solar pond systems.

Ibrahim Dincer is a Full Professor in the Faculty of Engineering and Applied Science at the University of Ontario Institute of Technology in Oshawa, Canada. He has chaired many national and international conferences, symposia, workshops and technical meetings. He has delivered many keynote and invited lectures. He is an active member of various international scientific organisations and serves as editor-in-chief, associate editor, regional editor and editorial board member on various prestigious international journals. He is a recipient of several research, teaching and service awards.

1 Introduction

Thermal Energy Storage (TES) is one of the key technologies for energy conservation, and therefore, it is of great practical importance. One of its main advantages is that it is best suited for heating and cooling thermal applications. A salinity-gradient solar pond is an integral collection and storage device of solar energy. By virtue of having built-in TES, it can be used irrespective of time and season. In an ordinary pond or lake, when the sun's rays heat up the water, this heated water, being lighter, rises to the surface and loses its heat to the atmosphere. The net result is that the pond water remains at nearly atmospheric temperature. The solar pond technology inhibits this phenomenon by dissolving salt into the bottom layer of this pond, making it too heavy to rise to the surface, even when hot. The salt concentration increases with depth, thereby forming a salinity gradient. The sunlight which reaches the bottom of the pond remains entrapped there. The useful thermal heat is then withdrawn from the solar pond for applications (Dincer and Rosen, 2011).

Recently, increasing attention has been paid to environmentally benign and sustainable energy sources, e.g. solar energy and related applications. In this regard, solar ponds and solar collectors appear to be a potential solution for implementation. Solar ponds and collectors have some advantages and disadvantages. The biggest challenge is to reduce the heat losses during the storage period. On the other hand, solar pond heats up slowly but store heat in a longer period of time than solar collectors (Bozkurt and Karakilcik, 2012). Many studies have been done about solar pond and collectors (Karakilcik et al., 2006a; Karakilcik et al., 2006b; Smyth et al., 2006; Anderson et al., 2010; Alvarez et al., 2010; Karim et al., 2010; Karim et al., 2011; Kumar and Rosen, 2011; Moghadam et al., 2011). Some experimental and theoretical studies dealt with a solar pond integrated with different applications to increase performance of the solar pond (El-Sebaii, 2005; Velmurugan and Srithar, 2007; El-Sebaii et al., 2008; Akbarzadeh et al., 2009; Velmurugan et al., 2009; Singh et al., 2011). Exergetic performance assessment of a solar pond was first time studied by Karakilcik and Dincer (2008).

There have not been any experimental and theoretical investigations on exergetic performance assessment, through exergy efficiency, of the solar pond integrated with solar collectors. This was in fact the key motivation behind the present work. The present work then becomes the first work in the area dealing with the investigation of exergetic performance analysis of the Integrated Solar Pond (ISP) and comparison with the corresponding energy efficiency during the days of the month. In this work, an ISP was constructed and tested at Cukurova University in Adana, Turkey (i.e. 35°18′ E longitude, 37°05′ N latitude). Heat storage performance of the solar pond was increased by using flat-plate solar collectors in ISP. Heat energy was transferred to the solar pond storage zone through a heat exchanger system that was placed in storage zone. Experiments were carried out to determine heat storage, and the energy and exergy efficiencies of the integrated system for a particular rate of incident solar radiation and heat energy transferred from solar collectors. The energy and exergy efficiencies of the integrated system were determined and compared. The reference environment temperature is specified for exergy analysis as an average representative temperature.

2 System description

Generally solar ponds consist of three zones: The first zone, Upper Convective Zone (UCZ), is the fresh water layer at the top of the pond. This zone is fed with fresh water to maintain the cleanliness of the pond and replenish the lost water due to evaporation. The second zone, Non-Convective Zone (NCZ), is composed of salty water layers whose brine density gradually increases towards Heat Storage Zone (HSZ). The NCZ is an important insulated zone to the working of a solar pond. It allows an extensive amount of solar radiation to penetrate into the storage zone while inhibiting the propagation of long-wave solar radiation from escaping because water is opaque to infrared radiation. The third zone, HSZ is composed of the highest density. Considerable part of the solar energy is absorbed and stored by this bottom zone.

In this study, we measure density and temperature to determine the energy efficiency and compare it with the exergy efficiency of the ISP. Figure 1 shows a schematic representation of an integrated system, consisting of the cylindrical solar pond, heat exchanger and solar collectors. It is a novel solar pond system is called an ISP which consists of three main components. One is cylindrical solar pond with a radius of 0.80 m and a depth of 2 m, the bottom and the side walls of the pond were plated with the iron-sheets in 5 mm thickness, and in between with a glass wool of 50 mm thickness as the insulating layer. Another is heat exchanger as cylindrical serpentine and last one is four conventional flat-plate solar collectors with dimensions of 1.90 m × 0.90 m.

Figure 1 Integrated solar pond and collectors system

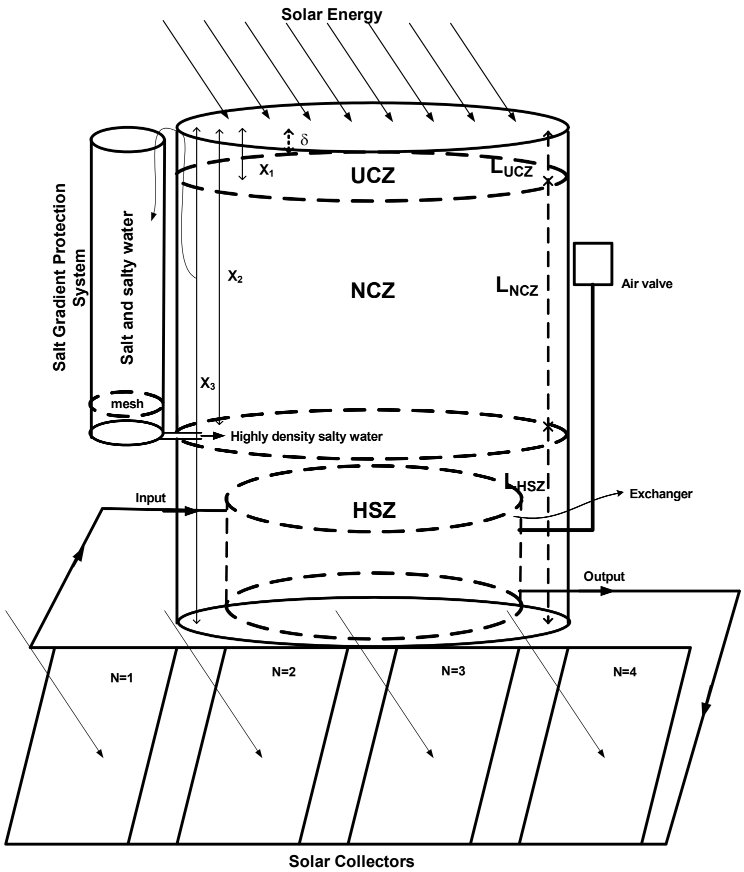

The cylindrical solar pond's inner zones possess different density levels of salty water. First, highly density salty water is prepared in the plastic tanks in order to form HSZ of the solar pond, and then the salty water is rested in the tanks up to a period of time until clarify before filled in HSZ. After finish the processing, the salty water is filled by pump through plastic hose up to NCZ. The thicknesses of the UCZ, NCZ and HSZ are 0.2, 0.8, 1 m, respectively. The range of salt gradient in the inner zones is such that the density is 1000–1030 kg/m^3 in UCZ, 1030–1165 kg/m^3 in NCZ and 1165–1185 kg/m^3 in HSZ. In this the main aim is prevented by convection heat losses from HSZ to NCZ and stored high amount of the solar energy by absorbing by this bottom region. Second, increasing densities the different densities salty water layers are created step by step by using a wood floating plate to protect the mixing of the below layers. NCZ is composed of salty water layers whose brine density gradually increases towards HSZ. Finally, the last zone is fed with fresh water in order to maintain its density as close as possible to the density of fresh water in the upper part and meet the water lost due to evaporation. As seen in Figure 1 this zone is called upper convective zone and X_1 is the height of UCZ. δ is the thickness (a few cm) of the upper layer of X_1 where long wave solar energy is absorbed. The second zone is non-convective zone between heat storage zone and UCZ. X_2 is the distance from bottom of NCZ to the surface, X_3 is the distance from bottom of HSZ to the surface, N is the number of collectors. The exchanger is composed of the cylindrical serpentine with a radius of 0.5 m and a height of 0.6 m and a thickness of 0.03 m.

The experimental temperature distributions were measured by using temperature sensors which are J-type thermocouple. These sensors were placed into the inner zones as well as the inlet and outlet of the heat exchanger. Hence, the temperature distribution profiles of these regions at any time were experimentally measured by a data acquisition system. To measure the temperature distributions of various regions, the temperature sensors were placed into the inner zones, starting from the bottom, at 0.10, 0.30, 0.50, 0.70, 0.90, 1.10, 1.30, 1.50, 1.70, 1.90 m heights. The data acquisition system was connected to a computer for data recording, monitoring and processing. The temperature of the inner layers of the pond, air and inlet-outlet of the heat exchanger were measured on an hourly basis throughout the months. The experimental density distributions were measured by using hydrometer. To measure the density distributions of various layers, the slim hoses were placed into the inner zones. The salty water samples of the layers were withdrawn through siphon and measured by using hydrometer.

The conventional flat-plate solar collectors are connected to the heat exchanger to transfer heat energy to store in HSZ of the solar pond. These are the most common solar collectors used in solar water-heating systems in homes and space heating systems. The flat-plate collector consists of an insulated metal box with a glass cover and a dark-coloured absorber plate. Solar radiation is absorbed by the absorber plate and transferred to a fluid that circulates through the collector in tubes. In an air-based collector the circulating fluid is air, whereas in a liquid-based collector it is usually water. Flat-plate collectors have the advantages of storing the heat energy very rapidly compared to solar ponds during the time in a day. However, their heat storage life time is shorter than that of solar pond. Therefore, energy stored using flat-plate collectors can be lost if it is not utilised with in a few days. On the other hand, solar pond can store the thermal energy for long-term storage.

3 Analysis

Exergy analysis is a method that uses the conservation of mass and conservation of energy principles together with the second law of thermodynamics for the design and analysis of systems and processes. The exergy method can be suitable for furthering the goal of more efficient energy-resource use, for it enables the locations, types and true magnitudes of wastes and losses to be determined. Therefore, exergy analysis can reveal whether or not, and by how much, it is possible to design more efficient energy systems by reducing the sources of inefficiency in existing systems. From the point of view of energy and exergy efficiency, it is important to note that if a fossil fuel-based energy source is used for a low-temperature thermal application like space heating or cooling, there would be a great difference between the corresponding energy and exergy efficiencies (Dincer, 1998).

An understanding of the relations between exergy and the environment may reveal the underlying fundamental patterns and forces affecting changes in the environment, and help researchers to deal better with environmental damage. Exergy analysis permits many of the shortcomings of energy analysis to be overcome. Exergy analysis acknowledges that, although energy cannot be created or destroyed, it can be degraded in quality, eventually reaching a state in which it is in complete equilibrium with the dead state (Dincer and Rosen, 2011). It appears to be a potential tool for design, analysis, evaluation and performance improvement of the ISP system. Figure 2 shows each of the zones and the respective exergy flows.

Figure 2 Exergy flows in the inner zones of the solar pond

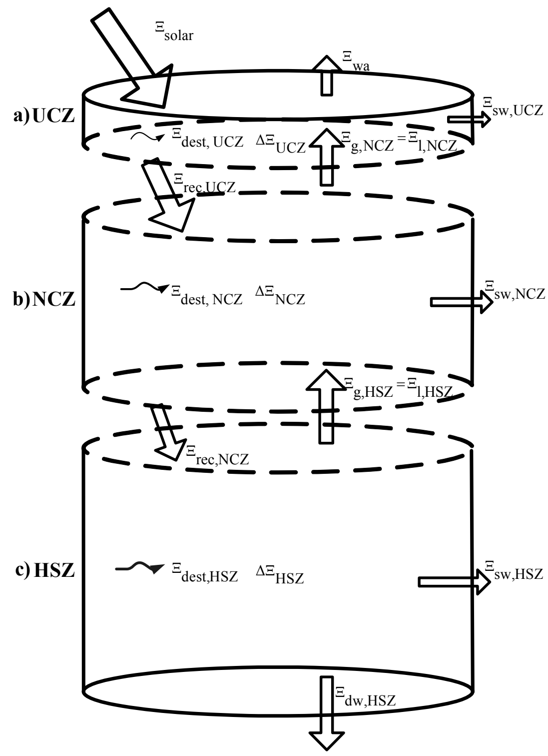

3.1 Energy analysis

The determination of heat storage energy is generally complicated due to the differences of inner and outer conditions (e.g. pond dimensions, salty water solutions, insulation, zone thicknesses, shading area of the layers, transmission and absorption characteristics for the layers). The heat energy was obtained experimentally in our system. Here, we consider the following key parameters: the temperatures in the solar pond and the incident radiation reaching on the surface of the pond and collectors. To calculate the heat storage energy of ISP, the temperature distribution of the zones should be measured. The temperature variations of layers depend on incident solar radiation on the horizontal surface, rates of absorption by the layers, local climate conditions, pond structure, time and insulation specifications. Temperature distributions of our system were obtained, experimentally. A part of the solar radiation incident on the solar pond is transmitted through UCZ and NCZ, after attenuation, to HSZ. Part of the transmitted solar radiation from NCZ to HSZ is reflected from the bottom and the majority of the solar radiation is absorbed in HSZ. So, HSZ temperature is increased and a temperature gradient develops in the zone.

The stored thermal energy in the storage zone of the ISP can be written as:

$$\Delta Q_{st} = Q_{in} - Q_{out} = Q_{solar} + Q_{FPC} - \left(Q_{up} + Q_{dw} + Q_{sw}\right) \tag{1}$$

where Q_{solar} is the total solar energy reaching the pond surface, Q_{FPC} is the incident solar energy reaching the absorber flat-plate surface, Q_{dw} is the total heat loss to the down wall from HSZ, Q_{up} is the heat loss from HSZ to NCZ. Q_{sw} is the total heat loss to the side wall of HSZ.

The energy efficiency of the ISP is given as

$$\eta_{ISP} = \frac{\Delta Q_{st}}{Q_{in}} = 1 - \frac{Q_{up} + Q_{dw} + Q_{sw}}{Q_{solar} + Q_{FPC}}$$
$$= 1 - \frac{\frac{k_{salt,w}A}{\Delta x_L}\left(T_{m,HSZ} - T_{m,NCZ}\right) + \frac{k_{dw}A}{\Delta x_{dw}}\left(T_b - T_a\right) + \frac{k_{sw}\, 2\,\pi\, r_{in} L_{HSZ}}{\Delta x_{sw}}\left(T_{m,HSZ} - T_a\right)}{\beta EA\left[\left(1-F\right)h\left(x-\delta\right)\right] + E\,(\tau\,\alpha)\,A_{FPC}^{N}} \tag{2}$$

where $k_{salt,w}$ is thermal conductivity of the salty water, A is the surface area of HSZ. Δx_L is the thickness of between HSZ and NCZ's middle point. $T_{m,HSZ}$ and $T_{m,NCZ}$ are the mean temperature of HSZ and NCZ, k_{dw} and k_{sw} are the thermal conductivity of the down and side wall, Δx_{dw} and Δx_{sw} are the thickness of down and side wall, respectively. T_b and T_a are the temperature of bottom and air temperature, respectively. r_{in} is the inner radius of the cylindrical solar pond. L_{HSZ} is the thickness of HSZ, E is the solar energy reaching the horizontal surface, A is the surface area of the pond, F is the absorbed energy fraction at a region of δ-thickness, h is the solar radiation ratio, A_{FPC}^{N} is the collector area, N is the number of collectors, τ is the transmission coefficient of the collector surface and α is the emissivity of the absorber surface of the flat-plate collector.

Also β is the fraction of the incident solar radiation that enters the pond, and is written using an expression (Hawlader, 1980):

$$\beta = 1 - 0.6\left[\frac{\sin\theta_i - \sin\theta_r}{\sin\theta_i + \sin\theta_r}\right]^2 - 0.4\left[\frac{\tan\theta_i - \tan\theta_r}{\tan\theta_i + \tan\theta_r}\right]^2 \tag{3}$$

where θ_i and θ_r are the angles of incidence and refraction.

The ratio of the solar energy reaching bottom of the pond (h) is given (Bryant and Colbeck, 1977) as:

$$h = 0.727 - 0.056\ln\left[\frac{(x_3 - \delta)}{\cos\theta_r}\right] \tag{4}$$

3.2 Exergy analysis

Here, we present a comprehensive exergy analysis of ISP with the exergetic efficiency. The exergy flows are well outlined in Figure 2.

The exergy of solar radiation can be expressed by as modified from Petala (2003):

$$\Xi_{solar} = E_{net}\left[1 - \frac{4T_0}{3T_S} + \frac{1}{3}\left(\frac{T_0}{T_S}\right)^4\right] \tag{5}$$

The exergy flows in HSZ are clearly shown in Figure 2 and the stored exergy equation in this regard results in:

$$\Delta\Xi_{st} = \Xi_{in} - \Xi_{out} = \Xi_{solar} + \Xi_{FPC} - \left(\Xi_{up} + \Xi_{sw} + \Xi_{dw} + \Xi_{dest}\right) \tag{6}$$

where Ξ_{in} is the input exergy including the exergy gained from flat-plate collector (Ξ_{FPC}). Ξ_{out} is the exergy lost from the pond, Ξ_{up} is the exergy loss from HSZ to NCZ, Ξ_{sw} is the exergy loss through side walls, Ξ_{dw} is the exergy loss through down wall and $\Xi_{dest,HSZ}$ is the exergy destruction in HSZ.

The exergy recovered in NCZ is given as:

$$\Xi_{rec,NCZ} = \Xi_{rec,UCZ} + \Xi_{g,HSZ} \tag{7}$$

$$\begin{aligned}\Xi_{rec,NCZ} = {} & E_{net} A_{net,UCZ}\left[1 - \frac{4T_0}{3T_S} + \frac{1}{3}\left(\frac{T_0}{T_S}\right)^4\right] + m_{m,NCZ} C_{p,m,NCZ} \\ & \left[\left(T_{m,NCZ} - T_{UCZ}\right) - T_a\left(\ln\frac{T_{m,NCZ}}{T_{UCZ}}\right)\right] + m_{m,HSZ} C_{p,m,HSZ}\left[\left(T_{m,HSZ\text{-}T} - T_{m,NCZ}\right) - T_a\left(\ln\frac{T_{m,HSZ}}{T_{m,NCZ}}\right)\right]\end{aligned} \tag{8}$$

where, $\Xi_{rec,UCZ}$ is the exergy recovered from NCZ and $\Xi_{g,HSZ}$ is the exergy gained from HSZ. E_{net} is the net solar radiation incident on UCZ of the pond. $A_{net,UCZ}$ is the net sunny area of UCZ. T_0 is the reference temperature, T_s is the sun's surface temperature taken as 6000 K. $C_{p,m,NCZ}$ and $C_{p,m,HSZ}$ are the average specific heat of salty water in NCZ and HSZ, respectively. $m_{m,NCZ} = \rho_{m,NCZ}V_{NCZ}$ is the mass of salty water in HSZ, $\rho_{m,HSZ}$ is the average density and V_{NCZ} is the volume of salty water in NCZ as $V_{NCZ} = 3.21$ m^3. $m_{m,HSZ} = \rho_{m,HSZ}V_{HSZ}$ is the mass of salty water in HSZ as given in Table 1; $\rho_{m,HSZ}$ is the averaged density and V_{HSZ} is the volume of salty water in HSZ as $V_{HSZ} = 4.02$ m^3. Table 1 shows average density, volume and mass of the zones.

Table 1 Average density, volume and mass of the zones

	HSZ	*NCZ*	*UCZ*
V (m^3)	4.02	3.21	0.80
ρ (kg/m^3)	1177.75	1084.08	1004.08
m (kg)	4733.61	3485.71	807.12

Here, Ξ_{FPC} is the exergy gained from solar collectors by using exchanger in the HSZ is given as

$$\Xi_{FPC} = \Xi_{solar}\ (\tau\,\alpha)\ A_{FPC}^{N} \tag{9}$$

The exergy losses, including exergy destruction within HSZ, can be derived as follows:

$$\Xi_{up} = m_{m,HSZ} C_{p,m,HSZ}\left[\left(T_{m,HSZ} - T_{m,NCZ}\right) - T_0\left(\ln\frac{T_{m,HSZ}}{T_{m,NCZ}}\right)\right] \tag{10}$$

$$\Xi_{sw} = m_{m,HSZ} C_{p,sw,HSZ}\left[\left(T_{m,HSZ} - T_{sw,HSZ}\right) - T_0\left(\ln\frac{T_{m,HSZ}}{T_{sw,HSZ}}\right)\right] \tag{11}$$

The exergy losses through side and down wall have a similar effect due to the fact that both outside walls have the same insulating materials and are surrounded by the ambient air.

$$\Xi_{dw} = m_{m,HSZ} C_{p,dw,HSZ} \left[\left(T_{m,HSZ} - T_{dw} \right) - T_0 \left(\ln \frac{T_{m,HSZ}}{T_b} \right) \right] \tag{12}$$

The exergy destruction in HSZ which can be written as

$$\begin{aligned} \Xi_{dest} &= T_0 \left(\Delta S_{net,HSZ} \right) = T_0 \left(\Delta S_{sys} + \Delta S_{surr} \right) \\ &= T_0 \left[m_{m,HSZ} C_{p,m,HSZ} \ln \frac{T_{m,HSZ}}{T_0} - \left(\frac{Q_{up}}{T_{m,HSZ}} + \frac{Q_{sw}}{T_0} \right) + \left(\frac{Q_{dw}}{T_0} \right) \right] \end{aligned} \tag{13}$$

where $\Delta S_{net,HSZ}$ is the net entropy change of HSZ.

We can now define the exergy efficiency for HSZ as the ratio of the exergy stored in HSZ to the total exergy input to HSZ which is essentially the exergy recovered from NCZ:

$$\psi_{HSZ} = \frac{\Delta\Xi_{st}}{\Xi_{in}} = 1 - \frac{\left(\Xi_{up} + \Xi_{sw} + \Xi_{dw} + \Xi_{dest.} \right)}{\Xi_{solar} + \Xi_{FPC}} \tag{14}$$

4 Results and discussion

In this work, we present the results of the model calculations for both energy and exergy efficiencies for each collector number in the ISP. The results were compared to show how exergy is crucial for determining true magnitudes of the losses taking place in HSZ and finding the true values by increasing the collector number of the solar pond. The stability of salt density distribution has a great significance as shown in Figure 3. It is some slight differences are observed between the density variation measured in a day due to essentially to increase of the collector number and to diffusion of the salt molecules. The primary reason for differences might be the increase in temperature in the upper layers of HSZ. This change originates from the thermophysical property of the salty water. This is eliminated by continuously adding fresh water to UCZ and increasing amount of the highly density salty water by starting the salt gradient protection system, as shown in Figure 1. It is well known that any reduction in salt gradient region decreases the pond's ability to store heat energy and hence increases the molecular diffusion flow.

In fact, Figure 3 shows the averaged experimental density variations of salty water versus the height of the pond from the bottom for using different number of collectors (e.g. 1, 2, 3 and 4). There are little differences between these density distributions measured for using one collector, due to the temperature changes and evaporation of salty water from the pond. As expected, increasing temperature decreases the density more for using four collectors. Generally, these changes can be eliminated by the salt gradient protection system.

The experimental temperature measurements were taken from integrated system in September. Solar collectors were used to increase temperature of HSZ. Experimental studies were performed using 1, 2, 3 and 4 collectors under approximately the same condition. One collector was used and temperature measurements were recorded from 09.00 to 17.00. To ensure approximately the same conditions HSZ was cooled to the starting temperature using cold water through heat exchanger system.

Figure 3 The variations of the salt density in the inner zones of the solar pond according to the number of collectors

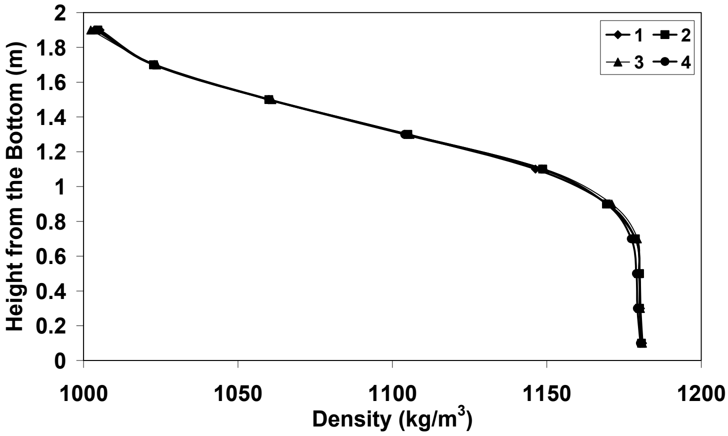

After obtaining approximately the same conditions the next day two collectors were used and also similar experiments were done for three and four collectors. Results are shown in Figures 4–7. It is clear that the zones temperature vary with each hour of the day, depending on the environment temperature, thermal energy transfer from collectors to HSZ and incoming solar incidence. The temperature of the zones generally increases with incident solar energy per unit area top of surface of the pond and collectors. There are heat losses from each zones, especially HSZ which affects the storage performance directly and drastically. In order to improve the performance and increase the efficiency, we should minimise the losses appropriately. Regarding the experimental temperature distributions in Figures 4–7 for the zones, as expected that the temperature of the UCZ, NCZ and HSZ are increased with the number of collector. As seen in Figures 6–7 although HSZ temperature distributions are sharply increased in a few hours, NCZ temperature distributions are slowly increased due to the thermophysical properties of water. The heat conduction coefficient of the water is low. Therefore, the heat transfer from HSZ to NCZ is occurred slowly.

Figure 4 Temperature distributions in the solar pond (for one collector)

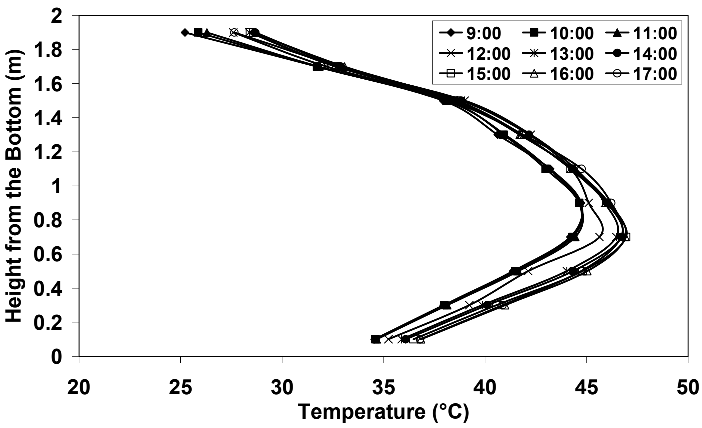

Figure 5 Temperature distributions in the solar pond (for two collectors)

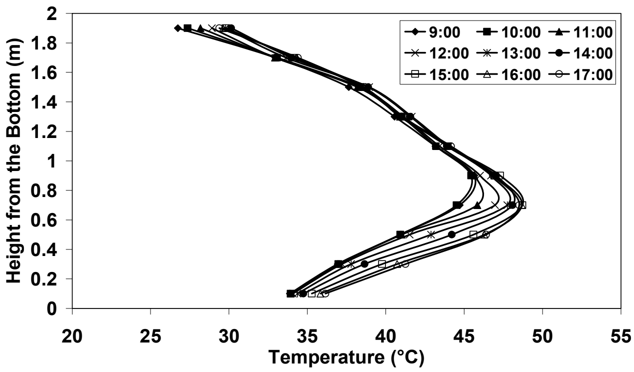

Figure 6 Temperature distributions in the solar pond (for three collectors)

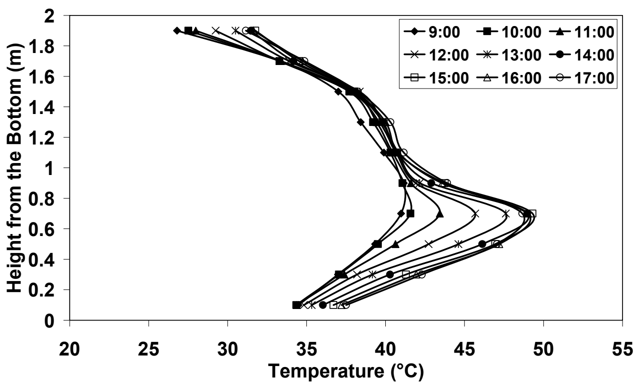

Figure 7 Temperature distributions in the solar pond (for four collectors)

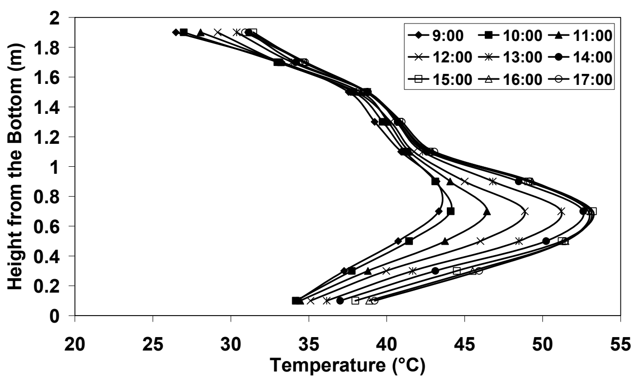

The solar energy data are obtained using a pyranometer from a local meteorological station. Figure 8 shows both averaged energy and exergy content variations in the inner zones of the pond versus months of the year, based on the experimental data. Reaching the solar radiation top of the surface of the UCZ is reflected, absorbed, and also part of portion is one recovered from UCZ for NCZ; and for HSZ it is the one recovered from NCZ. As seen in the figure, the exergy contents are less than the corresponding energy contents due to the fact that energy is conserved, but not exergy. Thus, some exergy is losses to the surrounding air, and exergy destructed in the each zones and collectors of the ISP. As seen in Figure 8, the lowest exergy contents appear in January and highest ones in July since the surrounding temperature of the integrated system plays a key role. It is important to mention that the shape of the energy and exergy content distributions follow the solar radiation profile closely.

Figure 9 shows the variation of the exergy input, exergy stored and destruction and losses taking place in the HSZ for using 1, 2, 3 and 4 collectors during the days in the September. The exergy content distributions were calculated using the reference environment temperatures, average mass flow rate, temperature distribution of heat exchanger and inner zones as listed in Table 2.

Figure 8 Energy and exergy distributions of the solar energy in Adana (Adana Meteorology Regional Offices, Turkey – 2010)

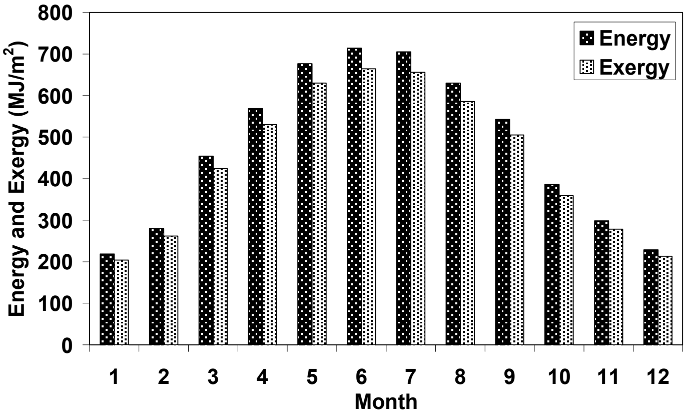

Figure 9 Variations of the exergy input, stored, destruction and losses of the integrated solar pond according to the number of collectors

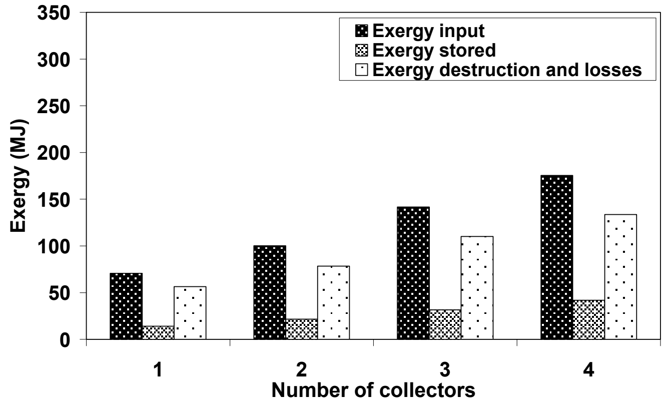

Table 2 Average temperature distribution of heat exchanger and inner zones, reference environment temperatures

N	*Inlet (°C)*	*Outlet (°C)*	*HSZ (°C)*	*NCZ (°C)*	*UCZ (°C)*	*Ref. Temp. (°C)*
1	48.18	34.04	41.07	40.36	27.41	28.43
2	49.74	33.32	40.89	40.64	28.88	28.05
3	53.26	34.63	41.24	38.90	29.78	27.66
4	57.18	35.86	43.67	40.24	29.53	27.28

As obviously seen here, the exergy inputs are equivalent to the summation of exergy stored and exergy destruction and losses. In this zone, we have exergy stored, instead of exergy recovered since the HSZ is the last zone, due to fact that this is why we run solar ponds to do daily and/or seasonal (or long-term) storage. The exergy stored becomes smallest compared to the exergy inputs and exergy destruction and losses in the HSZ, and appears to be maximum for using four collectors as 77.00 MJ and minimum for using one collector as 25.99 MJ, respectively. The values for using different collector's number are shown in Figure 9. It is important to mention that exergy destruction in the HSZ is caused by entropy generation directly which is a function of both entropy change within the system and entropy change in the surroundings due to the heat rejection. In both cases, the driving force for exergy destruction (or entropy generation) is the differences/changes between system and surrounding temperatures and pressures. In most cases, the pressure difference is negligibly small while the temperature difference is considerable.

The performance of the solar pond depends upon the total radiation reaching its surface. We used flat-plate solar collectors to increase surface area. In this way, the total radiations were increased and better solar pond performances were obtained. Figure 10 shows a comparison of both energy and exergy efficiencies and their variations based on the experimental data measured for using 1, 2, 3 and 4 collectors. The solar pond energy efficiencies were found to be 21.33%, 23.59%, 24.28% and 26.52% for using 1, 2, 3 and 4 collectors, respectively. Furthermore, the solar pond exergy efficiencies were found to be 20.02%, 21.66%, 22.24% and 23.84% for using 1, 2, 3 and 4 collectors, respectively. As shown in Figure 10, the differences between energy and exergy efficiencies are small for using 1, 2 and 3 collectors the largest for using four collectors.

Figure 10 Energy and exergy efficiency of the integrated solar pond according to the number of collectors

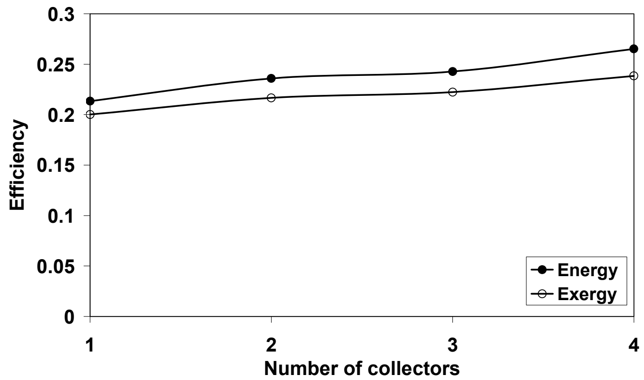

The number of collectors has an important effect on energy and exergy performance of the solar pond. As a result, the solar pond stores more exergy for using four collectors. The exergy destruction and losses significantly affect the performance of the pond and should be minimised to increase the system efficiency. Furthermore, the advantages of exergy analysis of such systems for design, analysis and performance improvement purposes are that it helps achieve the goal of more efficient energy resource utilisation, enabling locations, types and true magnitudes of wastes and losses to be determined.

5 Conclusions

In this paper we have studied performance analysis of a solar pond through exergy efficiency analysis. The exergy efficiencies calculated for using 1–4 collectors and the experimental data are compared with the corresponding energy efficiencies. As expected, the exergy efficiencies appear to be less than the energy efficiencies for the solar pond due to the exergy destructions in the zones and losses to the surroundings. It is important to determine the true magnitudes of these destructions and losses for performance improvement studies. Here, we carried out exergy calculations of ISP experimentally in order to demonstrate the effect of collectors on the performance of the solar pond. Therefore, the exergy efficiency of the ISP is an important parameter in practical applications.

Acknowledgements

The authors are thankful to University of Cukurova in Turkey for financial support of the present work (Grant No: FEF2004BAP4, FEF2009D2 and FEF2010BAP5) and University of Ontario Institute of Technology in Canada.

References

Akbarzadeh, A., Johnson, P. and Singh, R. (2009) 'Examining potential benefits of combining a chimney with a salinity gradient solar pond for production of power in salt affected areas', *Solar Energy*, Vol. 83, pp.1345–1359.

Alvarez, A., Cabeza, O., Muñiz, M.C. and Varela, L.M. (2010) 'Experimental and numerical investigation of a flat-plate solar collector', *Energy*, Vol. 35, pp.3707–3716.

Anderson, T.N., Duke, M. and Carson, J.K. (2010) 'The effect of colour on the thermal performance of building integrated solar collectors', *Solar Energy Materials & Solar Cells*, Vol. 94, pp.350–354.

Bozkurt, I. and Karakilcik, M. (2012) 'The daily performance of a solar pond integrated with solar collectors', *Solar Energy*, Vol. 86, pp.1611–1620.

Bryant, H.C. and Colbeck, I. (1977) 'A solar pond for London', *Solar Energy*, Vol. 19, p.321.

Dincer, I. (1998) 'Thermodynamics, exergy and environmental impact', *Proceedings of the ISTP-11 the 11th International Symposium on Transport Phenomena*, Hsinchu, Taiwan, pp.121–125.

Dincer, I. and Rosen, M.A. (2011) *Thermal Energy Storage Systems and Applications*, 2nd ed., Wiley, NY.

El-Sebaii, A.A. (2005) 'Thermal performance of a shallow solar-pond integrated with a baffle plate', *Applied Energy*, Vol. 81, pp.33–53.

El-Sebaii, A.A., Ramadan, M.R.I., Aboul-Enein, S. and Salem, N. (2008) 'Thermal performance of a single-basin solar still integrated with a shallow solar pond', *Energy Conversion and Management*, Vol. 49, pp.2839–2848.

Hawlader, M.N.A. (1980) 'The influence of the extinction coefficient on the effectiveness of solar ponds', *Solar Energy*, Vol. 25, pp.461–464.

Karakilcik, M. and Dincer, I. (2008) 'Exergetic performance analysis of a solar pond', *International Journal of Thermal Sciences*, Vol. 47, pp.93–102.

Karakilcik, M., Dincer, I. and Rosen, M.A. (2006a) 'Performance investigation of a solar pond', *Applied Thermal Engineering*, Vol. 26, pp.727–735.

Karakilcik, M., Kıymac, K. and Dincer, I. (2006b) 'Experimental and theoretical temperature distributions in a solar pond', *International Journal of Heat and Mass Transfer*, Vol. 49, pp.825–835.

Karim, C., Jomaa, S.M. and Akbarzadeh, A. (2011) 'A laboratory experimental study of mixing the solar pond gradient zone', *Solar Energy*, Vol. 85, pp.404–417.

Karim, C., Slim, Z., Kais, C., Jomaa, S.M. and Akbarzadeh, A. (2010) 'Experimental study of the salt gradient solar pond stability', *Solar Energy*, Vol. 84, pp.24–31.

Kumar, R. and Rosen, M.A. (2011) 'Integrated collector-storage solar water heater with extended storage unit', *Applied Thermal Engineering*, Vol. 31, pp.348–354.

Moghadam, H., Tabrizi, F.F. and Sharak, A.Z. (2011) 'Optimization of solar flat collector inclination', *Desalination*, Vol. 265, pp.107–111.

Petala, R. (2003) 'Exergy of undiluted thermal radiations', *Solar Energy*, Vol. 74, pp.469–488.

Smyth, M., Eames, P.C. and Norton, B. (2006) 'Integrated collector storage solar water heaters', *Renewable and Sustainable Energy Reviews*, Vol. 10, pp.503–538.

Singh, R., Tundee, S. and Akbarzadeh, A. (2011) 'Electric power generation from solar pond using combined thermosyphon and thermoelectric modules', *Solar Energy*, Vol. 85, pp.371–378.

Velmurugan, V., Pandiarajan, S., Guruparan, P., Subramanian, L.H., Prabaharan, C.D. and Srithar, K. (2009) 'Integrated performance of stepped and single basin solar stills with mini solar pond', *Desalination*, Vol. 249, pp.902–909.

Velmurugan, V. and Srithar, K. (2007) 'Solar stills integrated with a mini solar pond-analytical simulation and experimental validation', *Desalination*, Vol. 216, pp.232–241.

Nomenclature

A	surface area (m^2)
C	specific heat ($J\ kg^{-1}K^{-1}$)
E	total solar energy reaching to the pond (MJ/m^2)
F	absorbed energy fraction at a region of δ-thickness
h	solar radiation ratio
HSZ	heat storage zone
ISP	integrated solar pond
k	thermal conductivity (J/m°C)
L	thickness of the inner zones (m)
m	mass
N	number of collectors
NCZ	non-convective zone
Q	heat (J)
r	inner radius
T	temperature (°C)
UCZ	upper convective zone
X	thickness of inner zones (m)
V	volume

Greek Letters

η	energy efficiency
Ξ	exergy (J)
δ	thickness where long wave solar energy is absorbed (m)
α	emissivity of the absorber surface of the flat plate collector
β	incident beam entering rate into water
θ	angle (rad)
ρ	density (kg/m^3)
ΔS	entropy (J/K mol)
τ	transmission coefficient of the collector surface
Δx	thickness of horizontal layers (m)
ΔΞ	stored exergy (J)

ψ	exergy efficiency

Subscripts

a	ambient air
b	bottom
dest	destruction
dw	down wall
FPC	flat-plate collector
g	gained
HSZ	heat storage zone
i	incident
in	energy input
m	mean
NCZ	non-convective zone
net	net irradiation
out	energy output
r	refraction
rec	recovered
s	sun
solar	solar energy
st	heat stored inner zones of the pond
surr	surrounding
sw	side wall
sys	system
up	just above zone
w	fresh water.